Development 136, 161-171 (2009) doi:10.1242/dev.022087

A *Wnt7b*-dependent pathway regulates the orientation of epithelial cell division and establishes the cortico-medullary axis of the mammalian kidney

Jing Yu[1,*,‡], Thomas J. Carroll[1,†], Jay Rajagopal[1], Akio Kobayashi[1], Qun Ren[2] and Andrew P. McMahon[1,‡]

The mammalian kidney is organized into a cortex where primary filtration occurs, and a medullary region composed of elongated tubular epithelia where urine is concentrated. We show that the cortico-medullary axis of kidney organization and function is regulated by *Wnt7b* signaling. The future collecting duct network specifically expresses *Wnt7b*. In the absence of *Wnt7b*, cortical epithelial development is normal but the medullary zone fails to form and urine fails to be concentrated normally. The analysis of cell division planes in the collecting duct epithelium of the emerging medullary zone indicates a bias along the longitudinal axis of the epithelium. By contrast, in *Wnt7b* mutants, cell division planes in this population are biased along the radial axis, suggesting that *Wnt7b*-mediated regulation of the cell cleavage plane contributes to the establishment of a cortico-medullary axis. The removal of β-catenin from the underlying Wnt-responsive interstitium phenocopies the medullary deficiency of *Wnt7b* mutants, suggesting a paracrine role for *Wnt7b* action through the canonical Wnt pathway. *Wnt7b* signaling is also essential for the coordinated growth of the loop of Henle, a medullary extension of the nephron that elongates in parallel to the collecting duct epithelium. These findings demonstrate that *Wnt7b* is a key regulator of the tissue architecture that establishes a functional physiologically active mammalian kidney.

KEY WORDS: *Wnt7b*, Oriented cell division, Renal cortico-medullary axis, Collecting duct elongation, Loop of Henle elongation, Renal medulla, Mouse

INTRODUCTION

The functional renal circuitry comprises a long tubular epithelial network with distinct origins. The main body of the nephron derives from the metanephric mesenchyme, which epitheliarizes in response to Wnt inductive signals (Merkel et al., 2007). The ureteric epithelium arises from branching growth of the ureteric bud, which establishes the collecting duct network. The collecting duct system and nephrons of the mammalian kidney are organized along a renal cortico-medullary axis, such that different segments of nephrons and collecting ducts are spatially restricted within distinct cortical or medullary domains. The renal corpuscles and the convoluted tubules (proximal and distal) of the nephrons reside in the cortex (Little et al., 2007). The loop of Henle, which connects proximal and distal tubules of the nephron, extends into the medullary zone of the kidney, adjacent to the elongated tubular network of the collecting duct system (Little et al., 2007). The collecting duct epithelium also contains distinct cell types in cortical and medullary domains (Schuster, 1993). The cortico-medullary organization of the kidney is crucial for renal function; for example, the concentration of urine within the medullary compartment. However, the mechanisms that regulate cortico-medullary axis formation are unclear.

Our previous studies documented several Wnt family members that are expressed within subdomains of the developing mammalian kidney, and several of these regulate distinct renal developmental events (Carroll et al., 2005; Kispert et al., 1998; Kispert et al., 1996; Majumdar et al., 2003; Stark et al., 1994). *Wnt7b* encodes a Wnt ligand whose expression is restricted to the non-branching ureteric trunk component of the collecting duct system. Several studies have documented the actions of *Wnt7b* in multiple aspects of mammalian development, but its role in kidney development has not been addressed. *Wnt7b* signaling is crucial for placental, lung, eye, dendrite and bone formation (Lobov et al., 2005; Parr et al., 2001; Rajagopal et al., 2008; Rosso et al., 2005; Shu et al., 2002; Tu et al., 2007). In different tissues, *Wnt7b* functions via different branches of the Wnt signaling pathway, including the canonical Lef/β-catenin pathway (Lobov et al., 2005; Wang et al., 2005), the non-canonical planar cell polarity (PCP) pathway (Rosso et al., 2005), and the newly described G protein-linked PKC delta pathway (Tu et al., 2007). We demonstrate here that *Wnt7b* is essential for the establishment of the cortico-medullary axis of the mammalian kidney through the regulation of cell cleavage planes within the collecting duct epithelium. Mechanistic analyses suggest that *Wnt7b* acts indirectly by activating a canonical Wnt signaling pathway in an interstitial mesenchyme cell intermediate that coordinates the elongation of epithelial tubular networks forming the medullary zone.

MATERIALS AND METHODS

Tissue preparation

For BrdU labeling, pregnant female mice were injected with 0.5 mg BrdU/10 g body weight 2 hours before the harvesting of embryonic kidneys. For histological staining, immunofluorescent staining of paraffin sections, and in situ hybridization of frozen sections, tissues were fixed in 4% paraformaldehyde (PFA) at 4°C for 24 hours. For immunofluorescent analysis of frozen sections, tissues were fixed in 4% PFA or 2% PFA for 1 hour at 4°C. For vibratome section immunofluorescent staining, freshly

[1]Department of Molecular and Cellular Biology and Harvard Stem Cell Institute, Harvard University, 16 Divinity Avenue, Cambridge, MA 02138, USA. [2]Department of Cell Biology, University of Virginia, 1340 Jefferson Park Avenue, Charlottesville, VA 22908, USA.

*Present address: Department of Cell Biology, University of Virginia, 1340 Jefferson Park Avenue, Charlottesville, VA 22908, USA
†Present address: University of Texas Southwestern Medical Center at Dallas, 5323 Harry Hines Boulevard, Dallas, TX 75390, USA
‡Authors for correspondence (e-mails: jy4m@virginia.edu; amcmahon@mcb.harvard.edu)

Accepted 28 October 2008

dissected kidneys were fixed in 4% PFA at 4°C for 30 minutes, and then embedded in 15% gelatin/PBS (phosphate-buffered saline). After solidifying for 30 minutes at 4°C, gelatin blocks were fixed in 4% PFA at 4°C for 2 hours.

Histology and immunostaining

Paraffin blocks were sectioned at 6 μm for Hematoxylin and Eosin staining as described by Yu et al. (Yu et al., 2002). Frozen sections were sectioned at 12 μm. Gelatin blocks for vibratome sectioning were sectioned at 75 μm. Sections were blocked in blocking buffer (3% BSA, 1% normal donkey serum, PBS/0.1% Triton X-100) for 1 hour at room temperature and then incubated overnight at 4°C in primary antibodies diluted in blocking buffer. After washing in PBS/0.1% Triton X-100, sections were incubated in secondary antibodies diluted in blocking buffer at room temperature for 2 hours for frozen sections or at 4°C overnight for vibratome sections. Sections were then stained with Hoechst 33342 for 5 minutes, post-fixed with 4% PFA for 20 minutes at room temperature, and mounted with Vectashield mounting media (Vector Laboratories) with Hoechst 33342. TUNEL staining was performed with the ApopTag Red In situ Apoptosis Detection Kit (Chemicon International), following the manufacturer's instructions. Primary cilia immunostaining was visualized with a Personal DeltaVision microscope (Applied Precision). Three-dimensional projections were generated from stacks of optical sections. Other images were collected with a Zeiss LSM510 Axioplan 2 confocal microscope. For quantification of cell proliferation and apoptosis, 300-1600 cells from two to four sections of each kidney were counted. Primary antibodies used in this study were as follows: anti-phospho-histone H3 (Upstate Cell Signaling), anti-pan cytokeratin (Sigma), anti-BrdU (BD Pharmingen), anti-acetylated α-Tubulin (Sigma), anti-Polaris (gift of Dr B. K. Yoder, University of Alabama at Birmingham), anti-Cdh6 (gift of Dr G. Dressler, University of Michigan, Ann Arbor), anti-Umod (Biomedical Technologies), DBA-biotin (Sigma), anti-p57Kip2 (Neomarkers), anti-Lef1 (Santa Cruz), anti-β-galactosidase (Cappel), anti-Integrin α3 (gift of Dr J. Kreidberg, Children's Hospital, Boston), and anti-E-Cad (Zymed).

lacZ staining and vibratome sectioning

Freshly dissected kidneys were fixed in 4% PFA at 4°C for 1 hour. Kidneys were stained in *lacZ* staining solution at 4°C overnight. After post-fixing in 4% PFA, kidneys were embedded in 15% gelatin/PBS to make vibratome blocks. Three hundred micrometer (E13.5) and 150 μm (other stages) vibratome sections were dehydrated through a graded methanol series and cleared in benzyl alcohol:benzyl benzoate (1:1) for photography.

In situ hybridization with digoxigenin-labeled riboprobes

Frozen blocks were sectioned at a thickness of 16 μm. In situ hybridization was performed as described by Little et al. (Little et al., 2007). Briefly, sections were treated with 10 μg/ml proteinase K for 10 minutes, and hybridized with 500 ng/ml digoxigenin-labeled riboprobes overnight at 68°C. After the first post-hybridization wash, sections were treated with 2 μg/ml RNase for 15 minutes at 37°C. Sections were incubated in anti-DIG-AP antibody (1:4000, Roche) at 4°C overnight. After incubation with BM purple to visualize signals, sections were fixed in 4% PFA/0.2% glutaraldehyde and mounted in glycergel mounting media (DAKO).

Measurement of mitotic angles

Fifty micrometer frozen sections of E15.5 kidneys were immunostained with anti-phospho-histone H3 and anti-pan cytokeratin antibodies. Stacks of confocal optical sections were collected, from which three-dimensional reconstructions were generated with Imaris software. Mitotic angles were measured according to Fischer et al. (Fischer et al., 2006). Briefly, in three-dimensional reconstructions, the poles of each of the two anaphase chromosome clusters were marked as measurement points P1 and P2 with Imaris software. The *x*, *y* and *z* coordinates of the two points were then acquired with the Imaris software for generation of the vector of the mitotic division axis. Two points (P3, P4) on the collecting ducts harboring the anaphase cell were taken to generate the vector of the longitudinal axis of the collecting duct epithelium. The coordinates of the four points were used to calculate the angles between the vector of the mitotic division axis and the vector of the longitudinal axis of the collecting duct epithelium, the mitotic angle. Mann-Whitney U tests were performed for statistical significance of the distribution of mitotic angles between control and *Wnt7b* mutant samples.

RESULTS

The renal medulla fails to form in the absence of *Wnt7b* function

A number of Wnt genes are expressed with distinct spatial and temporal patterns within the mammalian metanephric kidney and regulate diverse aspects of kidney development (Merkel et al., 2007). *Wnt7b* expression is restricted to the Wolffian duct-derived ureteric trunk epithelium that gives rise to the collecting duct network and ureter of the urinary system (Fig. 1A-C), but is excluded from the ureteric tips. *Wnt7b* null mice die at embryonic day 9.5 (E9.5), before the onset of major organogenesis, as *Wnt7b* is essential for placental development (Parr et al., 2001). To genetically dissect *Wnt7b* functions in organ formation, we placed loxP sites on either side of exon3 of the *Wnt7b* gene (Wnt7b^{c3}) (Rajagopal et al., 2008), generating a Cre-dependent conditional null allele. As expected, when *Wnt7b* function was removed from both extra-embryonic and embryonic tissues by Cre-mediated recombination, embryos homozygous for this allele were phenotypically identical to those harboring the previously described *Wnt7b* null allele (Parr et al., 2001).

To bypass the embryonic lethality that results from the placental function of *Wnt7b*, *Wnt7b* activity was specifically removed from the mouse epiblast lineage by using the *Sox2Cre* driver line (Hayashi et al., 2002). The resulting *Wnt7b$^{c3/-}$; Sox2Cre* progeny (hereafter referred to as *Wnt7b* mutants) displayed a hypoplastic lung phenotype, were unable to breathe and died shortly after birth (Rajagopal et al., 2008). Histological examination of E18.5 kidneys revealed a striking phenotype: a complete absence of the renal medulla (Fig. 1J,K). In a wild-type kidney at this stage, the renal corpuscles are separated from the renal pelvis by the elongated epithelial network of the medullary region (Fig. 1J, arrow). By contrast, renal corpuscles abut the renal pelvis in *Wnt7b* mutants (Fig. 1K, arrow). Despite this pronounced medullary phenotype, the mutant kidneys were of a similar size to those of wild-type littermates: the average length of wild-type kidneys was 3.0±0.1 mm (n=3) and those of mutants 3.0±0.4 mm (n=4; P=0.90). Thus, the circumferential growth of the cortex, which is driven by branching morphogenesis of ureteric tips, did not appear to be compromised. Consistent with this interpretation, the mutant cortical region appeared histologically normal (Fig. 1K) and was similar in thickness to that of wild-type control kidneys when measured at the central-most plane (0.61±0.01 mm, n=4, versus 0.53±0.08 mm, n=3, respectively; P<0.17). Furthermore, the expression of an extensive set of markers of cortical development (*Wnt11*, *Wnt4*, *Foxd1*, *Gsh1*, *Slc34a1* and *Slc12a3*) that assessed ureteric branching, nephron induction and nephron patterning were represented normally in the cortical region of medullary-deficient *Wnt7b* mutant kidneys at E15.5 (Fig. 2). That the size of the kidney and the thickness of the renal cortex are similar between wild-type and mutant kidneys at E18.5 in most cases demonstrated that the mutant renal pelvis occupied a similar volume to the control renal pelvis with a renal medulla in it. At E18.5, whereas all *Wnt7b* mutants showed a complete absence of the medullary region, less than one-third of mutants exhibited a hydroureter-like swelling of the pelvic region and ureter, and the expressivity of this phenotype varied considerably (data not shown). Thus, the enlarged-looking renal pelvic space in

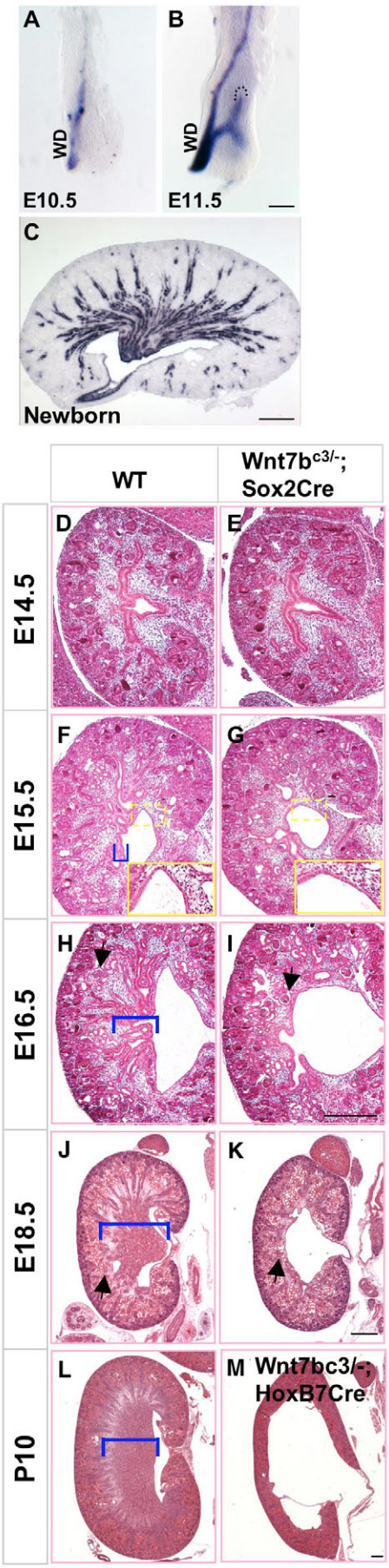

Fig. 1. *Wnt7b* is essential for the development of the medullary component of the mouse kidney. (**A-C**) In situ hybridization analysis of *Wnt7b* expression in the developing mouse kidney. Prior to ureteric bud outgrowth, *Wnt7b* mRNA was expressed at low levels in the mesonephric/Wolffian duct (WD) epithelium (A). After ureteric bud invasion into the metanephric mesenchyme, *Wnt7b* expression was restricted to the ureteric trunk epithelium (B) and its derivatives, the collecting duct epithelium and ureter of the kidney (C). Expression was not observed at the ureteric tips (boundary demarcated by dashed lines in B). Scale bars: 100 μm in A,B; 400 μm in C. (**D-M**) Hematoxylin and Eosin staining of kidney sections from wild-type littermates (D,F,H,J,L) and *Wnt7b* mutants (E,G,I,K,M) as indicated. The renal medullary compartment (bracketed) was first evident at E15.5 in wild-type embryos, but was absent from mutants at this and all later stages. The renal pelvis appeared normal (F and G, insets). Arrows in I and K point to renal corpuscles adjacent to the pelvic space. Arrows in panels H and J point to renal corpuscles that lie above the renal medulla. The P10 ureteric epithelium-specific *Wnt7b* mutants (M) exhibited hydroureter and hydronephrosis. Scale bars: 200 μm.

Wnt7b mutants does not appear to reflect an enlarged pelvis per se but rather the absence of the tubular epithelial network that demarcates the renal medulla.

To determine whether the observed renal phenotypes reflected a specific function for *Wnt7b* in the kidney and not a secondary consequence of *Wnt7b* signaling elsewhere in the embryo, a *Hoxb7Cre* driver line (Yu et al., 2002) was used to remove *Wnt7b* activity specifically within the nascent collecting duct epithelium. *Wnt7b*$^{c3/-}$*; Hoxb7Cre* embryos phenocopied the renal defects in *Wnt7b*$^{c3/-}$*; Sox2Cre* embryos at E18.5 (data not shown). Pups with a kidney-specific *Wnt7b* removal survived up to 11-12 days postpartum (P11-P12); however, the kidneys at this time were grossly abnormal and physiologically incompetent, which led to the postnatal death. Specifically, the urine osmolality of P10 *Wnt7b*$^{c3/-}$*; Hoxb7Cre* pups was only 56% that of wild-type littermates (see Fig. S2 in the supplementary material), which is consistent with a failure of medullary functions. Thus, kidney-specific removal of *Wnt7b* signaling demonstrates a direct action for the *Wnt7b* pathway in morphogenesis of the renal medulla and, as a consequence, the normal concentration of urine in this kidney compartment.

To determine whether the absence of a renal medullary compartment at E18.5 results from a failure of or a delay in renal medulla formation, or from a loss of the structure after the initiation of renal medulla formation, we analyzed a developmental series of wild-type and *Wnt7b* mutant embryos. No medullary compartment was evident in wild-type E14.5 embryos (Fig. 1D), but a medullary domain emerged between E15.5 and E16.5 (Fig. 1). The first evidence of an elongating tubular epithelium separating the renal cortex from the renal pelvis was evident at E15.5 (bracketed in Fig. 1F). By E16.5, a converging elongated tubular network of the renal medulla was a prominent feature of kidney organization (Fig. 1H). Wild-type and *Wnt7b* mutants were indistinguishable at E14.5 (Fig. 1D,E); however, the nascent renal medulla of the wild-type was absent from *Wnt7b* mutant kidneys at E15.5 (Fig. 1F,G). This phenotype became markedly more pronounced by E16.5 (Fig. 1H,I). No renal medulla was evident either in *Wnt7b*$^{c3/-}$*; Hoxb7Cre* mutant kidneys, even at P10 (Fig. 1L,M). In summary, *Wnt7b* signaling is essential for establishing the renal medulla of the mouse kidney. In this, *Wnt7b* appears to play a primary role in the establishment of a cortico-medullary axis of epithelial organization.

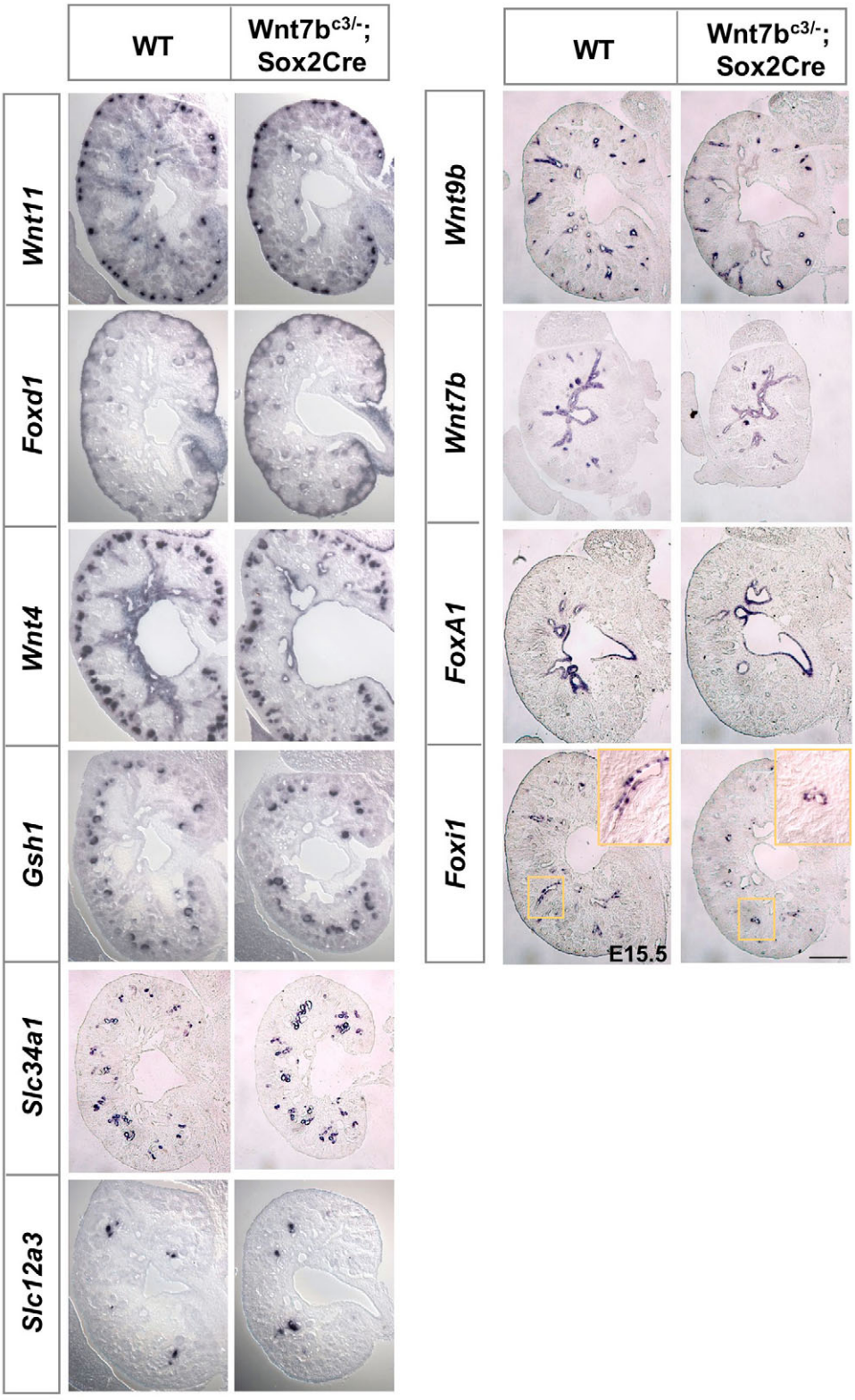

Fig. 2. Development of the renal cortex and patterning of the ureteric bud epithelium are normal in *Wnt7b* mutants. In situ hybridization to E15.5 kidney sections to examine branching morphogenesis (*Wnt11*), nephrogenesis (*Wnt4*), cortical stroma progenitors (*Foxd1*), nephron number and nephron patterning (*Gsh1* for podocytes, *Slc34a1* for proximal convoluted tubules, and *Slc12a3* for distal convoluted tubules) indicates that these processes were unaffected in *Wnt7b* mutants. The expression of *Wnt11* at the branching tips of the ureteric epithelium, *Wnt9b* in the non-tip ureteric epithelium, *Wnt7b* in the more-distal ureteric epithelium, renal pelvic epithelium and ureter, *Foxa1* in the prospective medullary collecting ducts, renal pelvic epithelium and ureter, and *Foxi1* in intercalated cells of the maturing collecting duct demonstrate normal stratification and differentiation of the ureteric epithelium in *Wnt7b* mutants. The *Wnt7b* riboprobe was generated from part of the exon 4 sequence and thus detected *Wnt7b* mRNA signals in both control and *Wnt7b* mutant kidneys. Scale bar: 200 μm.

Wnt7b regulates orientation of cell divisions in renal medullary collecting duct epithelium

The epithelial components of the renal medulla comprise medullary collecting ducts derived from the ureteric trunks and extensions of the loop of Henle, renal tubular components of the main body of the nephron. The major structure driving renal medulla formation appears to be the collecting duct epithelium, because compartmentalization of the renal cortex and renal medulla is evident in the absence of the loop of Henle in severe hypomorphs of *Fgf8* signaling (Grieshammer et al., 2005; Perantoni et al., 2005) and following nephron-specific removal of the transcriptional regulator *Lim1* (Kobayashi et al., 2005). Therefore, we focused our initial

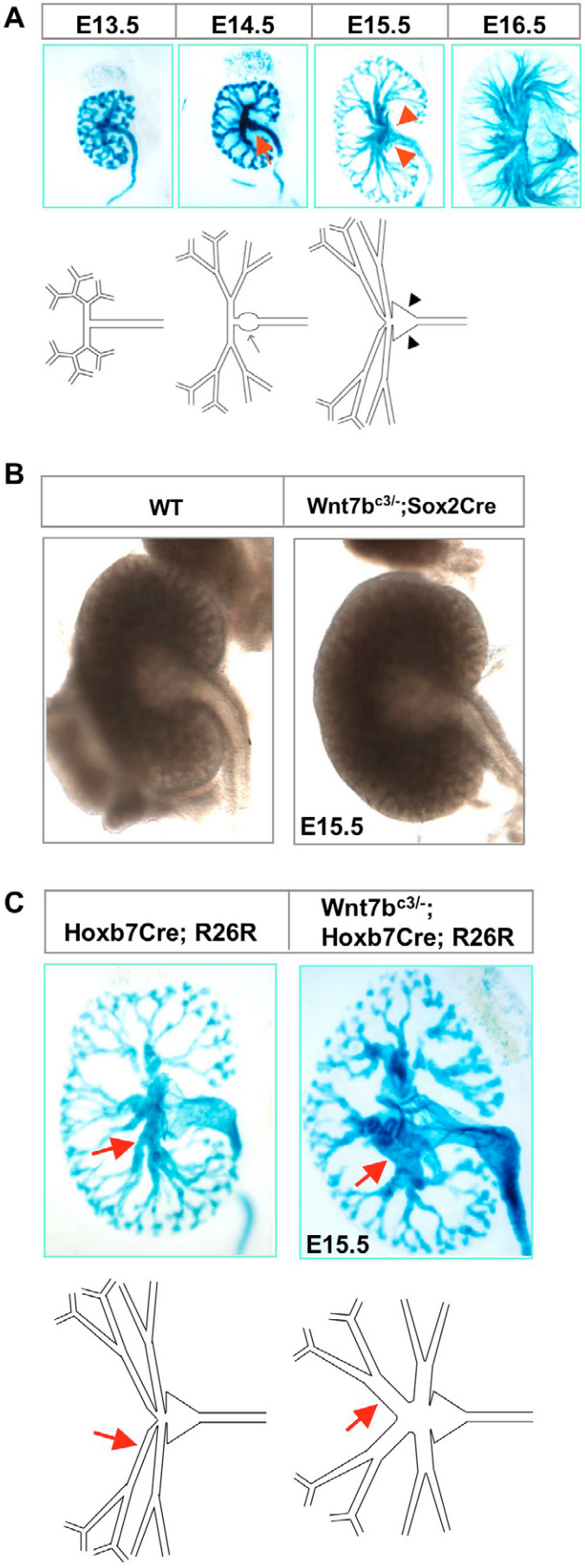

Fig. 3. Morphogenesis of the distal collecting duct epithelium is disrupted in *Wnt7b* mutants. (**A**) The organization of the developing collecting duct network was visualized through ureteric epithelium-specific, histochemical staining for *E. coli* β-galactosidase activity in wild-type kidneys from *Hoxb7Cre;R26R* embryos. Data represent thick (150-300 μm) vibratome sections at the stages indicated and are schematized in the panel below. Arrows highlight a swelling at the intersection between the ureter and the collecting duct epithelium; arrowheads indicate the triangular-shaped renal pelvis. (**B**) An analysis of freshly dissected kidneys showed that the ureter was not dilated in *Wnt7b* mutants at E15.5. (**C**) By contrast, the collecting duct epithelium was dilated in the prospective medullary region of *Wnt7b* mutants at E15.5 when the R26R reporter was activated in the context of the collecting duct network of the *Wnt7b* mutant kidney. Arrows indicate prospective medullary collecting ducts.

analysis on the ureteric bud-derived collecting duct epithelium to understand the mechanisms of normal renal medulla formation and the role of *Wnt7b* signaling in this process.

New ureteric epithelium is generated in part through the branching growth at the cortical tips of the ureteric network. The cortical tip-specific expression of *Wnt11* mRNA provides a general means of assessing both the normal regulation of the genetic circuitry governing tip growth and the number of branch tips within the kidney at any given stage. At E14.5, expression of *Wnt11* was not noticeably different in *Wnt7b* mutant kidneys when compared with wild-type littermates; similar numbers of branching events were observed and *Wnt11* was appropriately restricted to the tip region (Fig. 2; see also Fig. S3 in the supplementary material). A further analysis of cortical-medullary stratification of gene expression within the ureteric epithelium also demonstrated appropriate expression of two other Wnt family members: *Wnt9b* throughout much of the collecting duct epithelium except the tips and the distal-most region and ureter; and *Wnt7b* itself in more distal regions of the collecting ducts and the pelvic and ureteral transitional epithelium (Fig. 2). *Foxa1*, a novel marker we recently identified (Little et al., 2007) of more distal epithelia in the presumptive medullary collecting duct region and the pelvic and ureteral transitional epithelium, was expressed as expected in the mutant (Fig. 2). Finally, *Foxi1* demarcates intercalated cells, a differentiated cell type specific to the collecting duct epithelium; its normal expression in mutant kidneys demonstrates that the epithelium also differentiated as expected (Fig. 2). Thus, the failure of renal medullary formation was unlikely to result from either a mis-patterning or a mis-specification of the epithelial network of the developing collecting duct system.

To develop a better understanding of the dynamic organization of the renal medullary collecting ducts, we genetically labeled the collecting ducts combining the Cre-dependent β-gal-producing R26R mouse line (Soriano, 1999) with the ureteric epithelium-specific *Hoxb7Cre* strain (Fig. 3). Reorganization was observed in both the organization of the proximal ureter and the distal collecting duct network in conjunction with renal medulla development. The appearance of the future renal pelvis was preceded at E14.5 by a swelling at the proximal end of the ureter, at the intersection with the presumptive collecting duct epithelium (Fig. 3A, arrow). Within the latter, branches were approximately evenly spaced along the future cortico-medullary axis at E13.5, but appeared to elongate in the interbranch component of epithelium in the distal region close to the

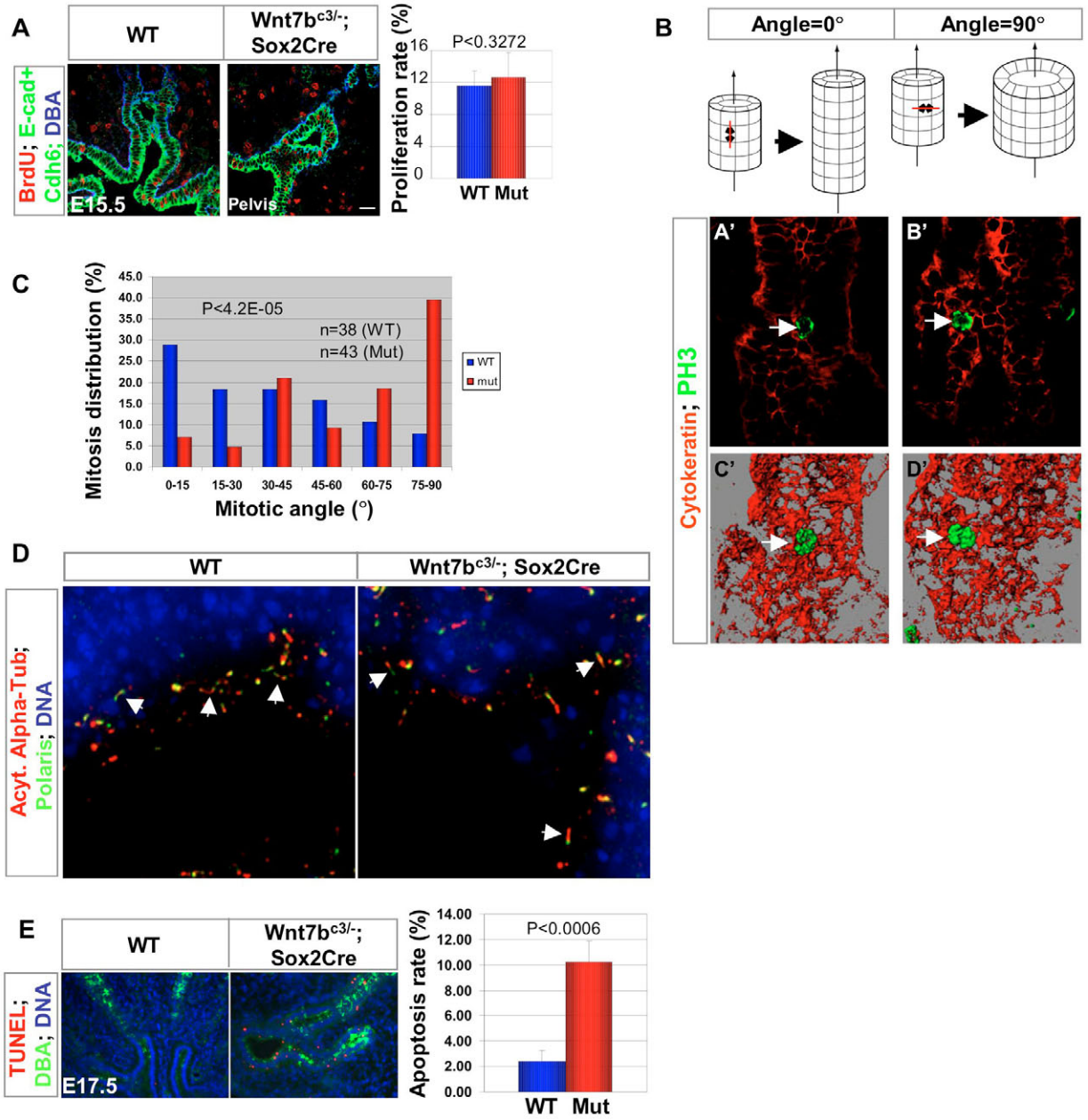

Fig. 4. The failure to initiate renal medulla development in *Wnt7b* mutants reflects alterations in the plane of epithelial cell division. (**A**) Cell proliferation was analyzed in wild-type and *Wnt7b* mutant kidneys at E15.5 by pulse-labeling with BrdU. BrdU incorporation was visualized by anti-BrdU antibodies in conjunction with specific markers, as indicated, to identify specific epithelial compartments. E-Cadherin (E-cad) and cadherin 6 (Cdh6) immunostainings together with DBA lectin demarcate the cell boundaries between the nephron and collecting duct epithelia. No significant difference in the proliferation rate is observed between wild-type (n=3) and *Wnt7b* mutants (n=4). Scale bar: 40 μm. (**B**) Diagrams illustrating the effects of oriented cell division on tubule morphogenesis and three-dimensional reconstructions of optical sections showing mitotic configurations in the collecting duct epithelium. Anaphase chromosomes were visualized with phospho-histone H3 staining (PH3, green, arrow) and the collecting epithelium with pan-cytokeratin staining (red; A′-D′). Stacks of single optical sections (A′,B′) were rendered to generate 3D images (C′,D′) for the measurement of mitotic angles. (**C**) Histogram of mitotic angles in the prospective medullary collecting ducts of wild-type and *Wnt7b* mutant kidneys at E15.5. Mitotic angles were determined relative to the longitudinal axis of the perspective collecting duct epithelium delineated with pan-cytokeratin immunostaining as detailed in the Materials and methods. (**D**) 3D reconstruction of stacks of optical sections of acetylated α-tubulin staining demonstrate that normally sized primary cilia (arrow) were present in the collecting duct epithelia of *Wnt7b* mutants. Moreover, the intraflagellar transport protein Polaris localized to the primary cilium as expected. (**E**) Apoptosis was compared by TUNEL analysis (red) in the collecting duct epithelium (DBA lectin, green) of kidney sections from wild-type and *Wnt7b* mutant embryos at E17.5. The apoptosis rate increased markedly and significantly in *Wnt7b* mutants (n=4) relative to in wild-type controls (n=4).

ureter by E14.5. This feature is consistent with the reported longitudinal growth of the ureteric trunk (Cebrian et al., 2004). This distended region continues to expand from E14.5 to E15.5 as the renal pelvic space is established. By E15.5, the ureteric trunks generated from the first few branching events orientate and extend in a spoke-like arrangement into, and centered on, the pelvic space, marking the

initiation of renal medulla formation (Fig. 3A). A high rate of proliferation within this region of the ureteric epithelium correlates with these events (Fig. 4A), suggesting that regional cell proliferation may play some roles in the formation of renal medulla. By E16.5, an elaborate network of ureteric branches funnels into the renal pelvic space, the typical architecture of the mature kidney structure.

The gross renal architecture was examined at E15.5 in wild-type and *Wnt7b* mutant littermates. In freshly prepared specimens (avoiding potential fixation artifacts), the ureter of mutants appeared normal and undilated [Fig. 3B; diameter of the wild-type ureter, 158.0±16.5 μm (n=6); diameter of the mutant ureter, 165.9±37.9 μm (n=6); P=0.63]. Histological analysis demonstrated that the renal pelvis was also comparable between wild-type and mutant kidneys (Fig. 1F,G, insets). However, whereas the collecting ducts in the nascent medullary region of wild-type embryos were long, thin epithelial tubes, those of *Wnt7b* mutants were considerably dilated and the branch points were less evident, most likely obscured by the epithelial dilation (Fig. 3C). These morphological disparities were observed even though the epithelium preserved a normal columnar, epithelial structure and cell proliferation was unaltered (Fig. 4A). Thus, neither rearrangement of cell shapes nor changes in the proliferative rate can readily account for the failure to establish a nascent medullary organization in *Wnt7b* mutants.

Oriented cell division has been postulated to regulate the appropriate growth of collecting duct epithelium in the postnatal kidney (Fischer et al., 2006). We explored the possibility that a *Wnt7b*-dependent orientated cell division event may normally regulate medullary morphogenesis. If collecting duct epithelial cells divide along the longitudinal axis of the duct (mitotic angle = 0 degrees), this orientated cell division would be expected to increase the length of the duct but not the circumference. If, on the contrary, cells divide along the radial axis of collecting duct (mitotic angle = 90 degrees), the duct is expected to increase in circumference, dilating rather than elongating (Fig. 4B). To determine the orientation of cell division in wild-type and mutant embryos, we measured mitotic angles of prospective medullary collecting duct cells as renal medulla formation initiates (E15.5). Phospho-histone H3 immunostaining was performed to visualize the mitotic configuration in collecting duct epithelium delineated by pan-cytokeratin staining (Fig. 4B). For accurate measurement, only the anaphase configuration was considered. As shown in Fig. 4C, the majority of wild-type cells (65.7%) divided along the longitudinal axis of the collecting duct epithelium (mitotic angles <45 degrees), whereas the majority of *Wnt7b* mutant cells (67.5%) divided along the radial axis of the collecting ducts (mitotic angles >45 degrees). The statistically significant difference in the bias of the plane of cell division may contribute to the shorter, wider ducts of *Wnt7b* mutant kidneys.

A re-orientation of cell division has recently been linked to cyst formation in the collecting ducts of mouse models of polycystic kidney disease (Fischer et al., 2006; Saburi et al., 2008), where the structure and/or action of the primary cilium is defective. By contrast, the primary cilium within the developing collecting duct network of *Wnt7b* mutants appeared grossly normal (Fig. 4D). Thus, the reorientation of the plane of cell division in *Wnt7b* mutants was not obviously linked to a cilia structural defect. Furthermore, proliferation and apoptosis, which were both elevated in most cystic kidneys, were not affected in collecting duct precursors in *Wnt7b* mutants at the onset of the renal medullary defect (E15.5), although apoptosis in the distal collect epithelium showed a fourfold increase in the mutants at E17.5 (Fig. 4A,E; see also Fig. S4 in the supplementary material). Thus, the only cellular property that we can identify that clearly correlates with the onset of the defects in epithelial organization in collecting ducts of *Wnt7b* mutant kidneys was the polarity of cell division.

Wnt7b signaling is essential for elongation of the loop of Henle

Another major epithelial component of the renal medulla is the loop of Henle, an intermediate segment of the nephron. At E18.5, the loop of Henle spans the entire length of the renal medulla (Fig. 5A). By contrast, the loop of Henle in *Wnt7b* mutant kidneys was truncated (Fig. 5B), resembling an earlier stage of development before it elongates to reach the junction between the renal cortex and renal medulla (Nakai et al., 2003). An analysis of segment-specific markers (*Slc12a1*, Barttin) showed that the arrest of loop of Henle elongation in the nephron primordium was not due to defects in loop of Henle specification (data not shown); rather, we observed a large and statistically significant reduction (84%) in cell proliferation in this structure in *Wnt7b* mutants (Fig. 5). Thus, *Wnt7b* activity is essential for coordinated growth of the loop of Henle, thereby establishing an appropriate medullary organization for the nephron.

Wnt7b signals to the adjacent interstitium via a canonical pathway

To understand the molecular mechanisms by which *Wnt7b* regulates renal medulla formation, we examined the medullary region for markers of Wnt signaling. *Lef1* and *Axin2*, two Wnt pathway components, are also common targets of canonical Wnt signaling. Interestingly, both genes displayed *Wnt7b*-dependent expression in medullary interstitial cells adjacent to the *Wnt7b*-expressing collecting duct epithelium (Fig. 6B), whereas their expression in other renal populations was unaltered (Fig. 6B; data not shown). These data suggest that at least one action of *Wnt7b* is to engage interstitial mesenchymal cells through a paracrine, canonical Wnt signaling pathway, a conclusion strengthened by the co-expression of Lef1 with a BAT-gal canonical Wnt reporter transgene (Maretto et al., 2003) in this mesenchyme population (see Fig. S5B in the supplementary material).

To determine whether this paracrine pathway might underpin *Wnt7b* function in renal medulla formation, we used a *Foxd1-Cre* line (*Foxd1GC*; A.K. and A.P.M., unpublished) to specifically remove β-catenin activity throughout the renal interstitium, including the sub-population of medullary interstitial cells (*Ctnnb1$^{c/-}$; Foxd1GC*, referred to as β-catenin interstitium mutants hereafter; see Fig. S6 in the supplementary material). Although β-catenin has a well-documented role in both canonical Wnt signaling and cell-cell adherens junctions in epithelia, in non-epithelial populations Wnt signaling appears to be its major activity. Remarkably, the removal of β-catenin from interstitial mesenchyme led to a failure in renal medulla development, and a loss of Lef1 and *Axin2* expression (Fig. 6A,B). By contrast, branching growth and nephron induction in the renal cortex was relatively normal, although the cortical region appeared to be somewhat thicker by histological analysis (0.52±0.02 mm, wild type versus 0.59±0.02 mm, mutant; P<0.002; n=4; Fig. 6A), a phenotype that may reflect additional roles for Wnt-dependent signaling within a non-medullary interstitial compartment. Together, these data lend strong support to the conclusion that canonical signaling within the interstitial mesenchyme plays a central role in mediating *Wnt7b* action in regulating renal medulla formation.

To date, only two interstitial regulators have been specifically linked to medullary development. *Pod1* (*Tcf21*) encodes a transcription factor expressed in the renal interstitium along with a number of other renal cell types (Quaggin et al., 1999). *Pod1*

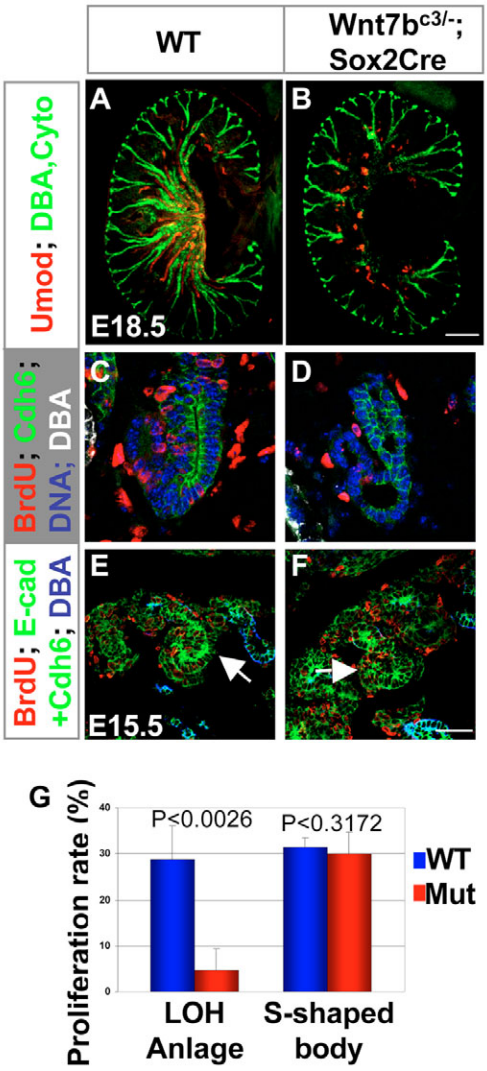

Fig. 5. *Wnt7b* is essential for coordinated growth of the loop of Henle, a medullary localized component of the developing nephron. (**A**,**B**) The loop of Henle was visualized in E18.5 kidney vibratome sections by immunostaining for Uromodulin (Umod, red). Sections are counterstained with DBA (green) to visualize the ureteric bud epithelium. The loop of Henle was greatly reduced in mutant kidneys compared with in wild-type littermates. (**C**,**D**) Measurement of BrdU incorporation in the loop of Henle anlagen at E15.5. The loop of Henle was identified as a U-shaped tubule in serial sections within the deeper cortex beneath the outer cortex where S-shaped bodies were localized. Loops of Henle of similar lengths were compared in the wild-type and mutant. (**E**,**F**) Measurement of BrdU incorporation in the S-shaped body (white arrows) at E15.5. (**G**) Cell proliferation was greatly reduced in the loop of Henle anlagen of mutants (P<0.0026). By contrast, no difference was observed between mutant and wild-type littermates at the S-shaped body stage (P<0.3172). S-shaped bodies were identified by immunostaining as being positive for E-cadherin (E-cad) and Cadherin 6 (Cdh6), but negative for DBA. The loop of Henle was positive for Cdh6 but negative for DBA. Scale bars: in B, 400 μm for A and B; in F, 40 μm for C-E.

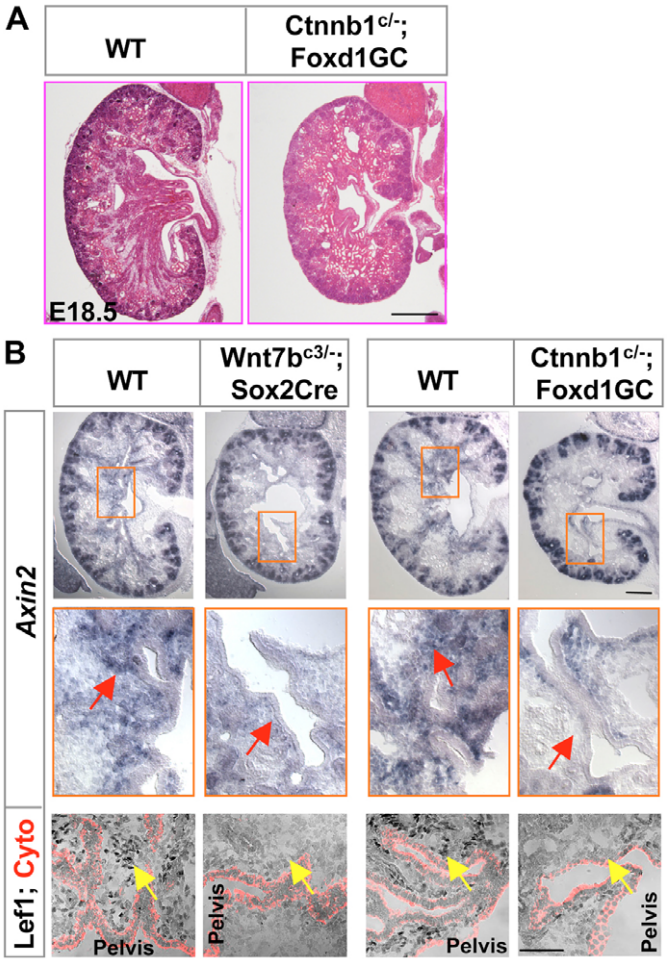

Fig. 6. *Wnt7b* signals to the adjacent interstitium through the canonical Wnt signaling pathway. (**A**) Hematoxylin and Eosin staining of E18.5 kidney sections following the removal of β-catenin activity from the renal interstitial mesenchyme. Mutant kidneys lack a renal medulla. Scale bar: 400 μm. (**B**) In situ hybridization (*Axin2*) and immunostaining (Lef1) on sections of E15.5 kidneys. A marked reduction was observed in *Axin2* mRNA and Lef1 protein expression within the interstitial mesenchyme positioned adjacent to the nascent medullary collecting ducts (arrows) following removal of β-catenin activity from this cell population. By contrast, their expression was not altered in other renal tissues. Cyto, cytokeratin. Scale bars: 200 μm in top four panels; 100 μm in all other panels.

knockout kidneys have no renal medulla, and *Pod1* mutant cells fail to contribute to medullary interstitium in chimeras with wild-type cells (Cui et al., 2003). However, expression of *Pod1* was not markedly altered in the renal interstitium of *Wnt7b* mutants (see Fig. S7 in the supplementary material). *p57Kip2* encodes a cyclin-dependent kinase (Cdk) inhibitor implicated in Beckwith-Wiedemann syndrome, whose expression in the renal interstitial cell compartment is restricted to a subset of interstitial mesenchyme in the renal medulla. The renal medulla, although present, is markedly reduced in *p57Kip2* mutants (Zhang et al., 1997). p57Kip2$^+$ cells co-localize with Bat-gal reporter-expressing cells indicating that p57Kip2$^+$ cells overlap with the mesenchymal canonical Wnt-target population (see Fig. S5C in the supplementary material). Interestingly, p57Kip2 expression was lost in this mesenchymal component in both *Wnt7b* and β-catenin interstitial cell mutants (Fig. 7), while Hoxa11, a more general marker of all renal interstitium, was still detected (Fig. 7; data not shown). Thus, p57Kip2 regulation may provide one direct link with *Wnt7b* function in elaboration of the renal medulla formation.

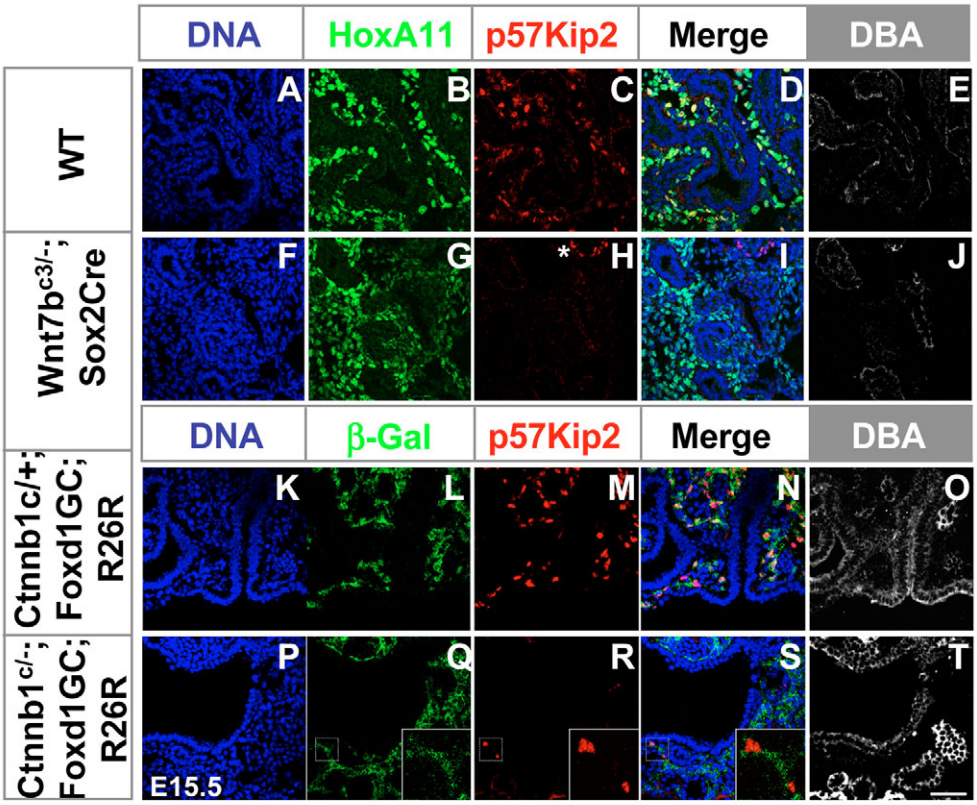

Fig. 7. p57Kip2 expression in mesenchyme cells of the medullary interstitium is dependent on a *Wnt7b* canonical signaling pathway. (**A-T**) The distribution of p57Kip2 was compared in E15.5 kidney sections from wild-type (A-E,K-O), *Wnt7b* mutants (F-J) and mutants lacking β-catenin within the interstitial mesenchyme (P-T). p57Kip2 protein was present in a subset of medullary interstitium within wild-type kidneys (nuclear staining in C,M). The interstitial expression of p57Kip2 was lost in this population in *Wnt7b* mutants (H), but was retained in podocytes (asterisk in H). By contrast, Hoxa11 was present throughout the renal interstitium of wild-type (B) and *Wnt7b* mutant (G) kidneys. When p57Kip2 was examined in interstitial cells of β-catenin interstitium mutants (β-galactosidase-positive from genetic labeling), p57Kip2 was not expressed in interstitial mesenchyme (R), except in rare cases where cells had escaped recombination (β-galactosidase-negative cells in insets in Q-S). Scale bar: 40 μm.

Wnt7b and ureter development

Wnt7b is expressed in the ureter epithelium and hydroureter was observed in some *Wnt7b* mutants at later stages, raising the possibility of a *Wnt7b* function in the ureter. However, we could find no evidence of a specific role of *Wnt7b* in ureter development. The histology of the mutant ureter appeared normal (data not shown). Furthermore, when dyes were injected into the mutant renal pelvic space at E18.5, the dyes accumulated in the bladder, demonstrating that the mutant ureter was not constricted and inserted into the bladder (see Fig. S8 in the supplementary material). In addition, when dyes were injected into the bladder, no vesico-ureteral reflux occurred in *Wnt7b* mutants (Fig. S8 in the supplementary material). Finally, sonic hedgehog signaling and smooth muscle differentiation were both normal (Fig. S8). Collectively, the data suggest that *Wnt7b* is not required for ureter differentiation. The hydroureter defect observed in a subset of *Wnt7b* mutants is likely to be a secondary complication of the medullary deficiencies.

DISCUSSION

Our work provides the first evidence that signaling by the ureteric epithelium establishes the cortico-medullary axis of the mammalian kidney. We identify *Wnt7b* as a key paracrine signaling factor in this process. *Wnt7b* is expressed exclusively in the non-branching collecting duct epithelium. Removal of *Wnt7b* activity leads to a failure of medullary development while other aspects of kidney development, notably ureteric branching and nephrogenesis, are unaffected. Canonical Wnt signaling targets are expressed in the subjacent interstitial mesenchyme, suggesting a paracrine signaling axis. Consistent with this view, expression of these targets is *Wnt7b* dependent. Additional support for canonical Wnt signaling in this interstitial population comes from the genetic removal of β-catenin in the renal interstitium. The resulting phenotype, an absence of the medullary area, closely resembles that caused by the loss of *Wnt7b* activity.

How then does *Wnt7b* action regulate this key morphogenetic process? The cellular and molecular basis of renal cortico-medullary axis formation is poorly understood. One early event that accompanies renal medulla formation is a significant longitudinal elongation of the renal medullary collecting ducts (Cebrian et al., 2004). One model implicates pelvic contractile forces in this process. In this, the smooth muscle-regulated peristaltic contractions and downward pulling forces from the renal pelvis may influence the longitudinal growth of the renal medulla. In this scenario, *Wnt7b* would act in some way to promote pelvic contraction, and in the absence of these contractions the pelvic region enlarges, which results in the failure of renal medulla formation. Several observations argue against this model. First, no pelvic enlargement was observed in *Wnt7b* mutants prior to the defects in renal medulla formation at E15.5. An enlarged renal pelvis was evident at later stages; however, whereas the failure of medullary development was fully penetrant, only 30% of *Wnt7b* mutants exhibited an expanded pelvic region. Furthermore, the removal of calcineurin (Ppp3r1 – Mouse Genome Informatics) from the pelvic and ureteral mesenchyme, or Angiotensin type 1 receptor (Agtr1a, Agtr1b – Mouse Genome Informatics) disrupts effective peristalsis, but a renal medulla forms and is normal at birth (Chang et al., 2004; Miyazaki et al., 1998). Both mutants display defective smooth muscle. Smooth muscle formation initiates at E15.5 in the kidney and ureter (Yu et al., 2002), and peristaltic contractions of the ureter and renal pelvis at a later stage. That the smooth muscle-based activity does not initiate medullary development is evident from sonic hedgehog mutants, where no smooth muscle forms at E15.5 but renal medullary development initiates normally (Yu et al., 2002).

Our study indicates that the emergence of the medullary region correlates with an elongation of the ureteric epithelium caused by a non-random plane of cell division. In this, new cells are added predominantly to a longitudinal axis of growth, as would be expected if the epithelium extends in a cortico-medullary direction. Strikingly, the failure of medulla formation in *Wnt7b* mutants correlates with a re-orientation of the cleavage plane, such that cells divide predominantly along the radial axis of the collecting duct. This shift in the orientation of cell division is expected to increase the circumferential growth and decrease longitudinal growth. Consistent with this view, a dilation of collecting duct epithelium was the only cellular defect we found associated with the onset of the failure of renal medulla formation in *Wnt7b* mutants (E15.5), although apoptosis was elevated at a later stage (E17.5). This suggests that oriented cell division is one crucial parameter initiating reorganization of the collecting duct epithelium to elongate the tubular network and establish the renal medulla. Cell death may play a later contributory role in the failure of renal medulla formation in *Wnt7b* mutants, but by this stage it is less clear whether increased apoptosis is a direct consequence of a failure of a *Wnt7b*-dependent regulatory function or a secondary consequence of phenotype-correlated defects; for example, a potential increase in intrapelvic pressure due to a higher volume of urine flow.

Oriented cell division has recently been demonstrated during postnatal renal collecting duct elongation (Fischer et al., 2006). In that process, cells also divide predominantly along the longitudinal axis of the duct. Thus, common mechanisms are employed throughout the extended period of kidney growth and development, although the control of orientated cell division is tighter postnatally. In polycystic kidneys, this longitudinal cell division is disrupted, such that cells divide randomly. A causal link is suggested of orientated cell division with polycystic kidney disease (PKD) etiology (Fischer et al., 2006; Saburi et al., 2008). In *Wnt7b* mutants, orientated cell division is also disrupted; however, unlike in PKD, the orientation of cell division appears to be such that cells tend to re-orientate to the plane opposite to that of wild-type cells. This difference may reflect additional regulatory inputs operating at the early stages; for example, a radial cleavage-promoting cue whose activity is masked by a dominant *Wnt7b* regulatory input. Alternatively, the PKD phenotype may result from a complete failure to sense any position-orientating cues, randomizing the cleavage planes within the collecting duct epithelium. Clearly, other tissues have specific pathways controlling the polarity of epithelial divisions, although these appear to be distinct from those reported here. For example, the removal of α-catenin or integrin β1 activity in skin leads to random cell division, whereas p63 mutants selectively disrupt asymmetric cell divisions (Lechler and Fuchs, 2005).

The primary cilium is a central structure in the etiology of PKD. Mutants that lack a primary cilium or primary cilium-associated proteins that mediate its signaling activity exhibit PKD (Lina and Satlinb, 2004; Siroky and Guay-Woodford, 2006; Yoder, 2007). Interestingly, unlike in polycystic kidneys, the primary cilium appears structurally normal in *Wnt7b* mutant kidneys, and is thus unlikely to play a similar role in the action of *Wnt7b*. Thus, differences in the structure or function of the primary cilium might be associated with the distinct defects in the orientation of cell division between PKD and *Wnt7b* mutants.

Tissue planar cell polarity (PCP) has been linked to the regulation of orientated cell division in the kidney and other tissue contexts (Baena-Lopez et al., 2005; Gong et al., 2004; Saburi et al., 2008). Thus, a Wnt/PCP pathway, where the relevant ligands might be regulated by *Wnt7b*, may be involved in the regulation of oriented cell division in renal collecting duct elongation. Although we cannot rule out an autocrine role for *Wnt7b* in the medullary collecting duct epithelium, our data indicate that the interstitial mesenchyme is a primary target of *Wnt7b* signaling, and removing the ability of these cells to respond to a canonical Wnt input replicates the *Wnt7b* mutant medullary phenotype. These interstitial cells lie in close proximity to the *Wnt7b*-secreting ureteric epithelium and express at least three Wnt ligands, *Wnt5a*, *Wnt4* and *Wnt11*. The expression of each of these is either absent or downregulated in a Wnt7b/β-catenin canonical Wnt signaling-dependent manner (see Fig. S7 in the supplementary material). Two of these Wnt ligands, *Wnt5a* and *Wnt11*, are predominantly associated with non-canonical planar cell polarity signaling, whereas *Wnt4* may act as both a canonical or a non-canonical ligand in a context-dependent manner. Thus, these Wnts are well placed to signal directly to the collecting duct epithelium. The medullary region develops in single mutants of *Wnt5a* and *Wnt11*. In *Wnt4* mutants, any medullary role would be obscured by the requirement for *Wnt4* in renal vesicle induction: loss of *Wnt4* leads to an early arrest in kidney development. Thus, compound mutants and novel genetic strategies will need to be generated to determine whether *Wnt7b* initiates a reciprocal Wnt/PCP signaling pathway from subjacent mesenchyme to stimulate longitudinal cell division in the overlying collecting duct epithelium. Furthermore, alternative models such as a non-PCP pathway of regulation or a more complex interplay between indirect mesenchymal and direct epithelial *Wnt7b* signaling cannot be ruled out. Genetic, cellular and biochemical strategies will be required to unravel this novel, critical regulatory interaction in organ biogenesis.

Pod1, *p57Kip2* and integrin α3 (*Itga3*) are three factors that have previously been shown to be involved in renal medulla morphogenesis. *Pod1* knockout kidneys have no renal medulla, whereas *p57Kip2* and *Itga3* knockout kidneys have a reduced renal medulla (Kreidberg et al., 1996; Quaggin et al., 1999; Zhang et al., 1997). Of these, only *p57Kip2* expression is lost in *Wnt7b* and β-catenin interstitium mutants (Fig. 7; see also Fig. S7 in the supplementary material), suggesting that *p57Kip2* may be a specific downstream target of *Wnt7b* signaling, whereas *Pod1* and *Itga3* may act in a parallel pathway or upstream of *Wnt7b*. Although *p57Kip2* is mainly known as a Cdk inhibitor, the kidney defects of *p57Kip2* null mice do not appear to directly associate with changes in cell proliferation (Zhang et al., 1997). Furthermore, several reports indicate Cdk inhibitor-independent activities for *p57Kip2* (Chang et al., 2003; Joseph et al., 2003; Yokoo et al., 2003). Importantly, a small renal medulla forms in p57Kip2 mutants. This phenotype is less severe than that of *Wnt7b* mutants, indicating that there are likely to be additional p57Kip2-independent targets of *Wnt7b* signaling.

Interestingly, the organizing function of *Wnt7b* also extends beyond the collecting duct epithelium to the nephron itself. Elongated growth of the loop of Henle is *Wnt7b* dependent; in the absence of *Wnt7b* action, little proliferative expansion of the loop of Henle anlage is observed. These data provide evidence for an ongoing role for ureteric epithelial signaling in nephron development downstream of *Wnt9b*-mediated induction of the nephron precursor (Carroll et al., 2005). In the loop of Henle anlagen, cell proliferation appears to be the crucial cellular response to *Wnt7b* functions. The different responses of loop of Henle and prospective medullary collecting duct epithelium to *Wnt7b* activities may result from tissue context-specific effects of a common signal downstream of *Wnt7b*, or from distinct downstream signals acting on the two epithelial tissues.

In summary, our data point to an integrated control of distinct epithelial networks through diverse cellular processes to generate a functional medullary compartment. In this, *Wnt7b* plays a pivotal role.

Its activity is essential for orientating cell cleavage in the collecting duct epithelium and for normal mitogenic activity in the loop of Henle. Furthermore, the data indicate that some, and possibly all, of these actions may be mediated through a hitherto neglected population of cells in our understanding of kidney development, the interstitial mesenchyme, highlighting the importance of this population in governing the spatiotemporal development of a vital component of functional kidney architecture, the renal medulla. Our findings provide a starting point to understanding how axial polarity in the mammalian kidney contributes to the establishment of a crucial axis of renal structure and function.

We thank Drs Jordan Kreidberg, Greg Dressler and Bradley Yoder for antibodies, and Dr Marco Pontoglio for the software for calculating the mitotic angles. We thank Joseph Bonventre and Ben Humphreys for advice on the measurement of urine osmolality. We thank anonymous reviewers for their constructive suggestions. Mary Duah provided assistance with the mouse colony breeding and genotyping analysis. This work was supported by a grant from NIH (DK054364) to A.P.M. A.K. was supported by fellowships from the National Kidney Foundation and an HSCI Seed Grant. Deposited in PMC for release after 12 months.

Supplementary material

Supplementary material for this article is available at
http://dev.biologists.org/cgi/content/full/136/1/161/DC1

References

Baena-Lopez, L. A., Baonza, A. and Garcia-Bellido, A. (2005). The orientation of cell divisions determines the shape of Drosophila organs. *Curr. Biol.* **15**, 1640-1644.

Carroll, T. J., Park, J. S., Hayashi, S., Majumdar, A. and McMahon, A. P. (2005). Wnt9b plays a central role in the regulation of mesenchymal to epithelial transitions underlying organogenesis of the mammalian urogenital system. *Dev. Cell* **9**, 283-292.

Cebrian, C., Borodo, K., Charles, N. and Herzlinger, D. A. (2004). Morphometric index of the developing murine kidney. *Dev. Dyn.* **231**, 601-608.

Chang, C. P., McDill, B. W., Neilson, J. R., Joist, H. E., Epstein, J. A., Crabtree, G. R. and Chen, F. (2004). Calcineurin is required in urinary tract mesenchyme for the development of the pyeloureteral peristaltic machinery. *J. Clin. Invest.* **113**, 1051-1058.

Chang, T. S., Kim, M. J., Ryoo, K., Park, J., Eom, S. J., Shim, J., Nakayama, K. I., Nakayama, K., Tomita, M., Takahashi, K. et al. (2003). p57KIP2 modulates stress-activated signaling by inhibiting c-Jun NH2-terminal kinase/stress-activated protein Kinase. *J. Biol. Chem.* **278**, 48092-48098.

Cui, S., Schwartz, L. and Quaggin, S. E. (2003). Pod1 is required in stromal cells for glomerulogenesis. *Dev. Dyn.* **226**, 512-522.

Fischer, E., Legue, E., Doyen, A., Nato, F., Nicolas, J. F., Torres, V., Yaniv, M. and Pontoglio, M. (2006). Defective planar cell polarity in polycystic kidney disease. *Nat. Genet.* **38**, 21-23.

Gong, Y., Mo, C. and Fraser, S. E. (2004). Planar cell polarity signalling controls cell division orientation during zebrafish gastrulation. *Nature* **430**, 689-693.

Grieshammer, U., Cebrian, C., Ilagan, R., Meyers, E., Herzlinger, D. and Martin, G. R. (2005). FGF8 is required for cell survival at distinct stages of nephrogenesis and for regulation of gene expression in nascent nephrons. *Development* **132**, 3847-3857.

Hayashi, S., Lewis, P., Pevny, L. and McMahon, A. P. (2002). Efficient gene modulation in mouse epiblast using a Sox2Cre transgenic mouse strain. *Gene Expr. Patterns* **2**, 93-97.

Joseph, B., Wallen-Mackenzie, A., Benoit, G., Murata, T., Joodmardi, E., Okret, S. and Perlmann, T. (2003). p57(Kip2) cooperates with Nurr1 in developing dopamine cells. *Proc. Natl. Acad. Sci. USA* **100**, 15619-15624.

Kispert, A., Vainio, S., Shen, L., Rowitch, D. H. and McMahon, A. P. (1996). Proteoglycans are required for maintenance of Wnt-11 expression in the ureter tips. *Development* **122**, 3627-3637.

Kispert, A., Vainio, S. and McMahon, A. P. (1998). Wnt-4 is a mesenchymal signal for epithelial transformation of metanephric mesenchyme in the developing kidney. *Development* **125**, 4225-4234.

Kobayashi, A., Kwan, K. M., Carroll, T. J., McMahon, A. P., Mendelsohn, C. L. and Behringer, R. R. (2005). Distinct and sequential tissue-specific activities of the LIM-class homeobox gene Lim1 for tubular morphogenesis during kidney development. *Development* **132**, 2809-2823.

Kreidberg, J. A., Donovan, M. J., Goldstein, S. L., Rennke, H., Shepherd, K., Jones, R. C. and Jaenisch, R. (1996). Alpha 3 beta 1 integrin has a crucial role in kidney and lung organogenesis. *Development* **122**, 3537-3547.

Lechler, T. and Fuchs, E. (2005). Asymmetric cell divisions promote stratification and differentiation of mammalian skin. *Nature* **437**, 275-280.

Lina, F. and Satlinb, L. M. (2004). Polycystic kidney disease: the cilium as a common pathway in cystogenesis. *Curr. Opin. Pediatr.* **16**, 171-176.

Little, M. H., Brennan, J., Georgas, K., Davies, J. A., Davidson, D. R., Baldock, R. A., Beverdam, A., Bertram, J. F., Capel, B., Chiu, H. S. et al. (2007). A high-resolution anatomical ontology of the developing murine genitourinary tract. *Gene Expr. Patterns* **7**, 680-699.

Lobov, I. B., Rao, S., Carroll, T. J., Vallance, J. E., Ito, M., Ondr, J. K., Kurup, S., Glass, D. A., Patel, M. S., Shu, W. et al. (2005). WNT7b mediates macrophage-induced programmed cell death in patterning of the vasculature. *Nature* **437**, 417-421.

Majumdar, A., Vainio, S., Kispert, A., McMahon, J. and McMahon, A. P. (2003). Wnt11 and Ret/Gdnf pathways cooperate in regulating ureteric branching during metanephric kidney development. *Development* **130**, 3175-3185.

Maretto, S., Cordenonsi, M., Dupont, S., Braghetta, P., Broccoli, V., Hassan, A. B., Volpin, D., Bressan, G. M. and Piccolo, S. (2003). Mapping Wnt/beta-catenin signaling during mouse development and in colorectal tumors. *Proc. Natl. Acad. Sci. USA* **100**, 3299-3304.

Merkel, C. E., Karner, C. M. and Carroll, T. J. (2007). Molecular regulation of kidney development: is the answer blowing in the Wnt? *Pediatr. Nephrol.* **22**, 1825-1838.

Miyazaki, Y., Tsuchida, S., Nishimura, H., Pope, J. C., Harris, R. C., McKanna, J. M., Inagami, T., Hogan, B. L., Fogo, A. and Ichikawa, I. (1998). Angiotensin induces the urinary peristaltic machinery during the perinatal period. *J. Clin. Invest.* **102**, 1489-1497.

Nakai, S., Sugitani, Y., Sato, H., Ito, S., Miura, Y., Ogawa, M., Nishi, M., Jishage, K., Minowa, O. and Noda, T. (2003). Crucial roles of Brn1 in distal tubule formation and function in mouse kidney. *Development* **130**, 4751-4759.

Parr, B. A., Cornish, V. A., Cybulsky, M. I. and McMahon, A. P. (2001). Wnt7b regulates placental development in mice. *Dev. Biol.* **237**, 324-332.

Perantoni, A. O., Timofeeva, O., Naillat, F., Richman, C., Pajni-Underwood, S., Wilson, C., Vainio, S., Dove, L. F. and Lewandoski, M. (2005). Inactivation of FGF8 in early mesoderm reveals an essential role in kidney development. *Development* **132**, 3859-3871.

Quaggin, S. E., Schwartz, L., Cui, S., Igarashi, P., Deimling, J., Post, M. and Rossant, J. (1999). The basic-helix-loop-helix protein pod1 is critically important for kidney and lung organogenesis. *Development* **126**, 5771-5783.

Rajagopal, J., Carroll, T. J., Guseh, J. S., Bores, S. A., Blank, L. J., Anderson, W. J., Yu, J., Zhou, Q., McMahon, A. P. and Melton, D. A. (2008). Wnt7b stimulates embryonic lung growth by coordinately increasing the replication of epithelium and mesenchyme. *Development* **135**, 1625-1634.

Rosso, S. B., Sussman, D., Wynshaw-Boris, A. and Salinas, P. C. (2005). Wnt signaling through Dishevelled, Rac and JNK regulates dendritic development. *Nat. Neurosci.* **8**, 34-42.

Saburi, S., Hester, I., Fischer, E., Pontoglio, M., Eremina, V., Gessler, M., Quaggin, S. E., Harrison, R., Mount, R. and McNeill, H. (2008). Loss of Fat4 disrupts PCP signaling and oriented cell division and leads to cystic kidney disease. *Nat. Genet.* **40**, 1010-1015.

Schuster, V. L. (1993). Function and regulation of collecting duct intercalated cells. *Annu. Rev. Physiol.* **55**, 267-288.

Shu, W., Jiang, Y. Q., Lu, M. M. and Morrisey, E. E. (2002). Wnt7b regulates mesenchymal proliferation and vascular development in the lung. *Development* **129**, 4831-4842.

Siroky, B. J. and Guay-Woodford, L. M. (2006). Renal cystic disease: the role of the primary cilium/centrosome complex in pathogenesis. *Adv. Chronic Kidney Dis.* **13**, 131-137.

Soriano, P. (1999). Generalized lacZ expression with the ROSA26 Cre reporter strain. *Nat. Genet.* **21**, 70-71.

Stark, K., Vainio, S., Vassileva, G. and McMahon, A. P. (1994). Epithelial transformation of metanephric mesenchyme in the developing kidney regulated by Wnt-4. *Nature* **372**, 679-683.

Tu, X., Joeng, K. S., Nakayama, K. I., Nakayama, K., Rajagopal, J., Carroll, T. J., McMahon, A. P. and Long, F. (2007). Noncanonical Wnt signaling through G protein-linked PKCdelta activation promotes bone formation. *Dev. Cell* **12**, 113-127.

Wang, Z., Shu, W., Lu, M. M. and Morrisey, E. E. (2005). Wnt7b activates canonical signaling in epithelial and vascular smooth muscle cells through interactions with Fzd1, Fzd10, and LRP5. *Mol. Cell. Biol.* **25**, 5022-5030.

Yoder, B. K. (2007). Role of primary cilia in the pathogenesis of polycystic kidney disease. *J. Am. Soc. Nephrol.* **18**, 1381-1388.

Yokoo, T., Toyoshima, H., Miura, M., Wang, Y., Iida, K. T., Suzuki, H., Sone, H., Shimano, H., Gotoda, T., Nishimori, S. et al. (2003). p57Kip2 regulates actin dynamics by binding and translocating LIM-kinase 1 to the nucleus. *J. Biol. Chem.* **278**, 52919-52923.

Yu, J., Carroll, T. J. and McMahon, A. P. (2002). Sonic hedgehog regulates proliferation and differentiation of mesenchymal cells in the mouse metanephric kidney. *Development* **129**, 5301-5312.

Zhang, P., Liegeois, N. J., Wong, C., Finegold, M., Hou, H., Thompson, J. C., Silverman, A., Harper, J. W., DePinho, R. A. and Elledge, S. J. (1997). Altered cell differentiation and proliferation in mice lacking p57KIP2 indicates a role in Beckwith-Wiedemann syndrome. *Nature* **387**, 151-158.